Recovery of acetate by anion exchange with consecutive CO_2-expanded methanol desorption

A model-based approach

Cabrera-Rodríguez, Carlos I.; Cartin-Caballero, Carlos M.; Platarou, Evgenia; de Weerd, Florence A.; van der Wielen, Luuk A.M.; Straathof, Adrie J.J.

DOI
10.1016/j.seppur.2018.03.068

Publication date
2018

Document Version
Final published version

Published in
Separation and Purification Technology

Separation and Purification Technology 203 (2018) 56–65

Contents lists available at ScienceDirect

Separation and Purification Technology

journal homepage: www.elsevier.com/locate/seppur

Recovery of acetate by anion exchange with consecutive CO_2-expanded methanol desorption: A model-based approach

Carlos I. Cabrera-Rodríguez[a], Carlos M. Cartin-Caballero[a,b], Evgenia Platarou[a], Florence A. de Weerd[a], Luuk A.M. van der Wielen[a,c], Adrie J.J. Straathof[a,*]

[a] Department of Biotechnology, Delft University of Technology, van der Maasweg 9, 2629 HZ Delft, The Netherlands
[b] Escuela de Química, Universidad Nacional de Costa Rica, Heredia, Costa Rica
[c] Bernal Institute, University of Limerick, Castletroy, Limerick, Ireland

ARTICLE INFO

Keywords:
Acetate
Anion exchange
Desorption
CO_2-expanded methanol
Ion exchange modeling

ABSTRACT

Production of bio-based acetate is commonly hindered by the high costs of the downstream processing. In this paper, a model is developed to describe a new method that recovers acetate salts using anion exchange resins, and subsequently desorbs and upgrades them using CO_2-expanded alcohol. The model consists of equilibrium parameters for both the adsorption and desorption step. The calculated parameters are: for the adsorption $K_{Cl^-}^{Ac^-} = 0.125$, $K_{Cl^-}^{HCO_3^-} = 0.206$ and $K_{OV,HAc} = 0.674 \frac{\text{mol / kg}_{\text{resin}}}{\text{mol / kg}_{\text{solution}}}$, and for the desorption $pK_{MeCO_3^-}^{Ac^-} = 3.71$. The maximum experimental concentration of acetic acid obtained in CO_2-expanded methanol is 0.427 mol/kg (20 g/L_{MeOH}) at an operating pressure of 31 bar. The model represents the expected trends for all species, and can be used to design a multicolumn system for the recovery and upgrading of carboxylates.

1. Introduction

Bio-based production of carboxylic acids via fermentation is a route to a wide variety of chemicals [1]. Examples of carboxylic acids that can be fermented from renewable materials, and for which large scale production exists, are acetic acid, citric acid, lactic acid, and itaconic acid [2]. Commercial production of carboxylic acids by fermentation is only possible if the recovery from the aqueous solution is efficient.

Some fermentation methods to produce carboxylic acids (concentrations 2–100 g/L) require titration with a base to maintain neutral pH, and as a result produce a carboxylate salt [2]. Traditional recovery of carboxylic acids from these carboxylate salts involves high energy consumption and waste co-production. One method to capture carboxylates from a dilute solution is to use strong anion exchange resins. Anion exchange resins are used to recover carboxylates because of the high affinity of the positively charged functional group. To avoid the use of strong mineral acids during desorption, a novel process for the recovery of carboxylic acid using the strong anion exchange resins and desorption with CO_2-expanded alcohols was developed [3]. At the end, the resin is regenerated to the bicarbonate form and the carboxylic acid dissolves in the CO_2-expanded alcohol solution for further processing (e.g. ester formation).

The main advantages of the method are: high solubility of CO_2 in the alcohol, no stoichiometric waste salt production (if the liberated bicarbonate is reused to control the pH of the fermentation), and integration with further downstream steps such as esterification, distillation or crystallization. The method was tested to work with different alcohols and carboxylates recovered from aqueous solutions and paper mill wastewater. However, the main limitation of the method is the high dilution of the produced carboxylates and esters (0.1–0.3 wt. %) after desorption/esterification [3,4]. A higher concentration of products in the CO_2-expanded alcohol solution would facilitate the further purification. However, no theoretical or empirical data are available to predict the maximum concentration achievable in desorption at a given amount of methanol and CO_2. For these reasons, a model that can predict the equilibrium concentration of carboxylate desorption using CO_2-expanded methanol is needed. In this paper, acetic acid is used as example for the determination of the model parameters. Acetic acid is one of the carboxylic acids that can be produced via fermentation. It is industrially used in the synthesis of vinyl acetate, cellulose acetate, and other acetate esters [5].

To predict the maximum achievable concentration during desorption, the current research aims to develop an equilibrium model for both the adsorption of aqueous acetate and chloride to a strong anion exchange resin in the bicarbonate form and subsequent desorption of acetic acid with CO_2-expanded methanol. After desorption with CO_2-

* Corresponding author.
E-mail address: A.J.J.Straathof@tudelft.nl (A.J.J. Straathof).

https://doi.org/10.1016/j.seppur.2018.03.068
Received 22 November 2017; Received in revised form 22 March 2018; Accepted 29 March 2018
Available online 07 April 2018

Nomenclature

a	Redlich-Kwong parameter (bar $K^{0.5}$ m^6 mol^{-2})
a_i	ion size parameter (nm)
A_c	column cross sectional area (m^2)
A	Debye-Hückel parameter for solvent ($kg^{0.5}$ $mol^{-0.5}$)
b	Redlich-Kwong parameter (kg/mol)
B	Debye-Hückel parameter for solvent ($mol^{-1/2}$ $kg^{-1/2}$ nm^{-1})
D_{app}	apparent dispersion (m^2 s^{-1})
f	fugacity (bar)
$HETP$	height equivalent to a theoretical plate (m)
I	ionic strength (mol kg^{-1})
k	reaction rate (s^{-1})
K_a	equilibrium constant acetic acid dissociation (Adimensional)
K_B^A	equilibrium constant of ion exchange (Adimensional)
K_{ACA}	dissociation constant of methyl carbonic acid (Adimensional)
$K_{CO_2,i}$	dissociation of carbonic acid or bicarbonate (Adimensional)
K_{HCO2}	partition constant of carbon dioxide in water (Adimensional)
K_m	dissociation constant in methanol (Adimensional)
K_{ov}	adsorption constant of acetic acid (mol kg_{resin}^{-1})/(mol $kg_{solution}^{-1}$)
K_1	partition constant of carbon dioxide in methanol (Adimensional)
L	packed length of column (m)
m	molal concentration (mol kg^{-1})
P	pressure (bar)
q	molal concentration in resin phase (mol kg^{-1})
q_{max}	maximum resin capacity (mEq g^{-1})
R	ideal gas constant (m^3 bar K^{-1} mol^{-1})
t	time (s)
t_0	characteristic time of tracer (s)
T	temperature (K)
u_{int}	interstitial velocity (m s^{-1})
v	molar volume (mol m^{-3})
$\dot{V}$	operating flow rate (m^3 s^{-1})
V_c	packed volume of column (m^3)
W	mass (g)
z	valence (Adimensional)

Greek

γ	activity coefficient in liquid phase (Adimensional)
$\gamma\pm$	mean activity coefficient (Adimensional)
ε	bed void fraction (m_{int}^3/m_{column}^3)
ϵ_r	dielectric constant (Adimensional)
ε_t	total column porosity (($m_{pore}^3 + m_{int}^3$)/m_{column}^3)
ρ	density (kg L^{-1})
τ	residence time of response peak in system with column (min)
τ_{col}	residence time of response peak in isolated column (min)
Φ	fugacity coefficient (Adimensional)

Subscript

A	component A
Ac^-	acetate ion
B	component B
eq	at equilibrium
Feed	feed to the column
H^+	hydrogen ion
HAc	acetic acid
HCl	hydrochloric acid
i	component i
in	inlet conditions
int	interstitial
j	component j
MeOH	methanol
$MeCO_3^-$	methyl carbonate ion
$MeCO_3H$	methyl carbonic acid
Res	resin
solv	solvent

expanded methanol, the resin is regenerated to the bicarbonate form. In this chapter, chloride is used as model anion to study the effect of impurities in the system. The equilibrium model is used to check the maximum concentration of acetate achievable in the CO_2-expanded methanol solution. Furthermore, an equilibrium dispersive model is used to model the transport through the column during adsorption and desorption. This mathematical model is needed for the design of a multicolumn system for the continuous recovery of carboxylates from diluted streams.

Table 1
Equilibrium expression and constants for the adsorption of acetate to a strong anion exchange resin.

Process	Equilibrium expression	Eq.	Parameter	Ref.
Acetic acid dissociation $HAc \leftrightarrow H^+ + Ac^-$	$K_{a,1} = \frac{\gamma_{H^+} \cdot m_{H^+} \cdot \gamma_{Ac^-} \cdot m_{Ac^-}}{\gamma_{HAc} \cdot m_{HAc}}$	(1)	$pK_{a,1} = 4.76$	[6]
Water dissociation $H_2O \leftrightarrow H^+ + OH^-$	$K_w = \gamma_{H^+} \cdot m_{H^+} \cdot \gamma_{OH^-} \cdot m_{OH^-}$	(2)	$pK_w = 14$	[7]
Bicarbonate dissociation $CO_2 + H_2O \leftrightarrow H_2CO_3$	$K_{HCO_2} = \frac{\gamma_{H_2CO_3} \cdot m_{H_2CO_3}}{f_{CO_2}}$	(3)	$pK_{HCO_2} = 2.77$	[7]
$H_2CO_3 \leftrightarrow H^+ + HCO_3^-$	$K_{CO_2,1} = \frac{\gamma_{H^+} \cdot m_{H^+} \cdot \gamma_{HCO_3^-} \cdot m_{HCO_3^-}}{\gamma_{H_2CO_3} \cdot m_{H_2CO_3}}$	(4)	$pK_{CO_2,1} = 3.6$	[7]
$HCO_3^- \leftrightarrow H^+ + CO_3^{2-}$	$K_{CO_2,2} = \frac{\gamma_{H^+} \cdot m_{H^+} \cdot \gamma_{CO_3^{2-}} \cdot m_{CO_3^{2-}}}{\gamma_{HCO_3^-} \cdot m_{HCO_3^-}}$	(5)	$pK_{CO_2,2} = 10.3$	[7]
Acetate ion exchange $Q^+Cl^- + Ac^- \leftrightarrow Q^+Ac^- + Cl^-$	$K_{Cl^-}^{Ac^-} = \frac{q_{Ac^-}}{q_{Cl^-}} \cdot \frac{\gamma_{Cl^-} \cdot m_{Cl^-}}{\gamma_{Ac^-} \cdot m_{Ac^-}}$	(6)	To be fitted	
Bicarbonate ion exchange $Q^+Cl^- + HCO_3^- \leftrightarrow Q^+HCO_3^- + Cl^-$	$K_{Cl^-}^{HCO_3^-} = \frac{q_{HCO_3^-}}{q_{Cl^-}} \cdot \frac{\gamma_{Cl^-} \cdot m_{Cl^-}}{\gamma_{HCO_3^-} \cdot m_{HCO_3^-}}$	(7)	To be fitted	
Acetic acid adsorption $Q^+Cl^- + HAc \leftrightarrow Q^+Cl^- \cdots HAc$	$K_{OV,HAc} = \frac{q_{HAc}}{\gamma_{HAc} \cdot m_{HAc}}$	(8)	To be fitted	

2. Theory

2.1. Ion exchange and adsorption equilibrium

In this study, recovery of acetate from a dilute aqueous solution at pH above the pK_a is performed using a strong anion exchange resin with a quaternary ammonium functional group (Type I). In addition to exchange of the acetate ion with the counter-ion of the resin's functional group, adsorption of the un-dissociated acetic acid to the resin backbone occurs. For this reason, the adsorption mechanism of acetic acid at a pH above the pK_a is described by ion exchange (Eq. (6)) and adsorption (Eq. (8)). The counter-ion of the functional group is chloride, and the interaction with acetate and bicarbonate (regenerated version of the resin) is studied. Additionally, the dissociations of all the species involved in the recovery of acetate are represented, and shown by the equilibrium reactions in Table 1, in which γ and m are the activity coefficient and molality in the aqueous phase, and q is the molality in the wet resin phase.

Ion exchange equilibria are described by a homogeneous mass action model, Eqs. (6) and (7). This originates from the common approach to treat the process like a reversible chemical reaction [8]. The exchanger is assumed to be a homogeneous phase, and non-idealities for the liquid phase are taken into account by introducing activity coefficients [9].

In this study, the activity coefficients for neutral species in solution are considered ideal (γ_{HAc} and $\gamma_{H_2CO_3} = 1$), since the deviation from ideality in aqueous systems is small and the error in the calculation is not significant [10]. For electrolyte solutions, deviations from ideality, even at low concentrations, can be important because of strong ion interactions with other ions, solvent and exchange resin. To quantify solution non-idealities, Debye-Hückel or Pitzer like models are generally used [11]. In this study, the activity coefficients for acetate, bicarbonate, carbonate, chloride, proton, hydroxide and sodium acetate in the water phase are calculated by the modified Debye-Hückel model of Truesdell and Jones (Eq. (9)) [7,12].

$$\log\gamma_i = \frac{-Az_i^2 I^{0.5}}{1 + Ba_i I^{0.5}} + b_i \mathrm{I} \tag{9}$$

The ionic strength, I, is calculated as Eq. (10), where z_i is the charge of ionic species.

$$I = \frac{1}{2}\sum_i m_i z_i^2 \tag{10}$$

The fermentation broths that we consider have an acetate concentration < 0.5 mol/kg, in which the Truesdell-Jones model is valid [12]. The parameters used for the activity coefficient model are reported in Appendix A.1 (Table A.1 and Table A.2).

The activity coefficients in the resin phase are resin dependent, and the simultaneous calculation of the activity coefficient and equilibrium constant exhibits a disturbing interdependence [9]. For this reason, it was assumed that the activity coefficients of the acetate, bicarbonate and chloride ions in the resin phase are approximately the same, leading to Eqs. (6) and (7) without activity coefficients in the resin phase.

For the non-dissociated acetic acid species, the adsorption is described through the linear region of the isotherm by a constant ($K_{OV,HA}$), Eq. (8).

All the parameters are calculated at 25 °C and 1 atm CO_2 and for this reason the fugacity coefficient (for the adsorption step) is assumed to be 1. The results of the batch adsorption experiments are used to calculate the selectivity and distribution coefficient for acetate, bicarbonate and acetic acid, respectively. The calculated parameters are further used to describe the effect of pH on the acetate and bicarbonate recovery. This information is used to model the recovery of the ions with the anion exchange resin at different pH and concentrations.

To solve the system, additional assumptions and mass balances are implemented:

- Electroneutrality in the liquid phase is assumed during all the experiments.

$$m_{H^+} + m_{Na^+} = m_{Cl^-} + m_{Ac^-} + m_{HCO_3^-} + 2\cdot m_{CO_3^{2-}} + m_{OH^-} \tag{11}$$

- The difference between inlet molalities and aqueous equilibrium molalities is assumed to be in the resin phase for each species i. In which W_{resin} is the mass of resin added in the liquid phase, and $W_{solution}$ is the mass of the solution, which are assumed to be constant. $q_{in,i}$ is the initial value of each species on the resin, which is $q_{in,i} = 0$, for most components except for one component in which $q_{in,i} = q_{max}$.

$$m_{in,i} + q_{in,i}\frac{W_{resin}}{W_{solution}} = m_{eq,i} + q_{eq,i}\frac{W_{resin}}{W_{solution}} \tag{12}$$

2.2. Desorption equilibrium

The anion exchange resin is regenerated using CO_2-expanded methanol as described in our previous publications [3,4]. However, in the current study no catalyst is used for the formation of esters, because the aim is to study the desorption equilibrium (without esterification). As a result, the desorption with CO_2-expanded methanol is described by five equilibrium reactions: the transfer of CO_2 from the gas to the methanol phase, the formation and deprotonation of methyl carbonic acid, the ion exchange of methyl carbonate with acetate and the protonation to acetic acid. Table 2 shows the equilibrium reactions considered in our desorption model.

In Table 2, CO_2 dissolution in methanol and acid formation were combined (Eq. (13)) [13]. The fugacity is calculated by Eq. (A.1) (Appendix A.2). The acetic acid dissociation in methanol was described using the published dissociation constant [14] (Eq. (16)), and converted to molality with ρ_{MeOH}.

For simplicity, the activity coefficients of neutral species are again taken as unity (γ_{HMeCO_3}, γ_{HAc}, γ_{MeOH}). The mean ionic activity coefficient, $\gamma_{\pm}$, is estimated using Eq. (17), which is the first term of Pitzer's model, as proposed by others [13], and used in Eqs. (14) and (16). This term of the Pitzer model includes the electrostatic far field interactions between

Table 2
Equilibrium expressions and constants for the CO_2 expanded methanol desorption of acetate.

Process	Equilibrium expression	Eq.	Parameter	Ref.
Methyl carbonic acid formation $MeOH + CO_2 \leftrightarrow MeCO_3H$	$K_1 = \frac{\gamma_{HMeCO_3}\cdot m_{HMeCO_3}}{\gamma_{MeOH}\cdot m_{MeOH}\cdot f_{CO_2}}$	(13)	$pK_1 = 3.21$	[13]
Methyl carbonic acid dissociation $MeCO_3H \leftrightarrow MeCO_3^- + H^+$	$K_{ACA} = \frac{m_{H^+}\cdot m_{MeCO_3^-}\cdot\gamma_{\pm}^2}{\gamma_{HMeCO_3}\cdot m_{HMeCO_3}}$	(14)	$pK_{ACA} = 5.73$	[13]
Ion Exchange $Q^+Ac^- + MeCO_3^- \leftrightarrow Q^+MeCO_3^- + Ac^-$	$K_{MeCO_3^-}^{Ac^-} = K_\gamma\frac{q_{MeCO_3^-}}{q_{Ac^-}}\cdot\frac{m_{Ac^-}}{m_{MeCO_3^-}}$	(15)	to be fitted	
Acetic acid dissociation $HAc \leftrightarrow H^+ + Ac^-$	$K_m = \frac{\rho_{MeOH}\cdot m_{H^+}\cdot m_{Ac^-}\cdot\gamma_{\pm}^2}{\gamma_{HAc}\cdot m_{HAc}}$	(16)	$pK_m = 9.63$	[14]

ions, but does not represent the specific binary, near-field interactions between pairs or ternary interactions (Ac^-, $MeCO_3^-$ and H^+), which are not reported elsewhere.

$$\ln\gamma_{\pm} = -A\left[\frac{\sqrt{I}}{1+1.2\sqrt{I}} + 1.67\cdot\ln(1+1.2\sqrt{I})\right] \quad (17)$$

A is the Debye-Hückel parameter; which is estimated as proposed by Gmehling et al. [15].

$$A(T) = 1.8248\cdot10^6\frac{kg^{0.5}}{mol^{0.5}}\frac{\sqrt{\frac{\rho_{solv}}{(kg/L)}}}{\left(\frac{T}{(K)}\epsilon_r\right)^{1.5}} \quad (18)$$

where ρ_{solv} is the density of methanol (0.786 kg/L), T is the temperature in K (298 K) and ϵ_r is the relative dielectric constant of methanol (33.05).

As previously, ion exchange equilibria for the batch experiments are described by a homogeneous mass action model. Since the mean activity coefficients of ions in the methanol phase are calculated by Eq. (17), the activity coefficients of acetate and methyl carbonate in methanol are equal. Furthermore, the activity coefficients of acetate and methyl carbonate on the resin phase are assumed to be the same. These assumptions lead to $K_\gamma = 1$ in Eq. (15). In this study, the mass action law model is derived to express the equilibrium concentration of acetic acid in methanol as a function of CO_2 pressure and the methanol/resin ratio. The concentration of anions in both phases are expressed in terms of acetic acid concentration, CO_2 pressure and methanol/resin ratio. Finally, the parameter $K^{Ac^-}_{MeCO_3^-}$ is determined from experimental data to model the ion exchange between acetate and methyl carbonate. Electroneutrality in the liquid phase is assumed in the batch calculations (Eq. (19), and the amount of each component bound to the resin is calculated as stated in Eq. (12).

$$m_{H^+} = m_{Ac^-} + m_{MeCO_3^-} \quad (19)$$

2.3. Dispersive model

The performance of a chromatographic column depends on factors that belong to two broad categories: equilibrium and dispersive factors. The equilibrium factors for our system have been described in Section 2.1 and 2.2. In this section, a term describing axial dispersion is included in the mass balance of the mobile phase, and the bed porosity is included [16,17]. In the model, the effect of several parameters are lumped into the dispersion coefficient D_{app}. The lumped parameter D_{app} includes peak broadening effects caused by the fluid dynamics of the packing (axial dispersion) and all other mass transfer effects. Using these assumptions, the differential mass balances for the liquid phase of all components are given by equation (20).

$$\frac{\partial m_i}{\partial t} = D_{app}\frac{\partial^2 m_i}{\partial x^2} - u_{int}\frac{\partial m_i}{\partial x} - \frac{1-\varepsilon}{\varepsilon}\left(\frac{\partial q_i}{\partial t}\right) \quad (20)$$

Here, the required parameters are the dispersion coefficient (D_{app}), the interstitial velocity (u_{int}) and the bed porosity (ε). The bed porosity is determined by residence time distribution experiments with potassium chloride and dextran as discussed in Section 3.5.1. It is further calculated using three characteristic times: the time of a tracer that enters the particles (t_{KCl}), the time of a tracer that should not enter the particles ($t_{Dextran}$) and the time of a tracer without column (dead volume until detector) ($t_{detector}$). In a typical experiment, t_{KCl} = 130s, $t_{detector}$ = 38s, and $t_{Dextran}$=117 s.

$$t_0 = t_{KCl} - t_{detector} \quad (21)$$

$$t_{0,int} = t_{Dextran} - t_{detector} \quad (22)$$

$$\varepsilon_t = t_0\frac{\dot{V}}{V_c} \quad (23)$$

$$\varepsilon = t_{0,int}\frac{\dot{V}}{V_c} \quad (24)$$

were $\dot{V}$ is the flow rate and V_c is the packed volume of the column, and calculated from the packed length and the internal diameter of the column. The interstitial velocity (u_{int}) is calculated from the operating flow rate ($\dot{V}$), the column internal cross-sectional area (A_c) and the extraparticle void fraction (ε) as:

$$u_{int} = \frac{\dot{V}}{A_c\cdot\varepsilon} \quad (25)$$

The dispersion coefficient (D_{app}) is calculated by moment analysis of an injection of potassium chloride and their relation with the van Deemter plot, and assumed to be the same for all components. The first two moments were calculated directly by numerical integration as:

$$\tau = \frac{\int_0^\infty m(t)\cdot t dt}{\int_0^\infty m(t)dt} \quad (26)$$

$$\sigma^2 = \frac{\int_0^\infty m(t)\cdot(t-\tau)^2 dt}{\int_0^\infty m(t)dt} \quad (27)$$

And the height equivalent to a theoretical plate (HETP) is calculated by the two moments and the column length (L_c) as:

$$HETP = \frac{\sigma^2_{col}\cdot L_c}{\tau^2_{col}} \quad (28)$$

Exploiting the connection between the apparent dispersion coefficient and the second moment, the dispersion coefficient can be calculated as proposed by others [17]. This apparent dispersion coefficient is used directly for the adsorption experiments. In the case of the desorption experiments, the apparent dispersion coefficient is calculated by fitting it to the experimental data.

$$D_{app} = \frac{HETP\cdot u_{int}}{2} \quad (29)$$

For the solid phase, the differential mass balance for each component is given by Eq. (30).

$$\frac{\partial q_i}{\partial t} = k(m_i - m_i^{eq}) \quad (30)$$

From which the m_i^{eq} is given by the specific equilibrium equation (Section 2.1, Eq. (12) and k for ion exchange is considered to be an instantaneous reaction (assumed to be 1000 s^{-1}). An additional required parameter is the total capacity of the resin (q_{max}), which is used to close the resin mass balance. The resin q_{max} is obtained experimentally as explained in Section 3.5.2.

The assumptions for all the experiments are:

- The feed is homogeneous so that the concentration of each species at the inlet is equal to $m_{i,feed}$ at all times.
- The apparent dispersion coefficient is equal for all species.
- The concentration of carbonate and carbonic acid are negligible at these conditions.

The initial and boundary conditions are:

- At time zero, the concentration of the binding component (acetate and chloride for adsorption, methyl carbonate for desorption) in the liquid phase throughout the column is zero.
- The concentration of bicarbonate (for adsorption) and acetate (for adsorption and desorption) was given a small initial concentration (0.01 mmol/kg) to avoid division by zero.
- The concentrations at the inlet were increased from zero to the feed value by using a step function.
- At the outlet boundary, a zero gradient of the liquid concentration was assumed.

- For adsorption, the resin phase was initially assumed to be fully loaded with bicarbonate and this is equal to q_{max}.
- For desorption, the methyl carbonic acid inlet concentration is assumed to be constant at the operating pressure of 31 bar CO_2. This was calculated with Eq. (13) and the result is shown in Table A.3.
- For desorption, the resin phase was initially assumed to be fully loaded with acetate (acetate loading) or with acetate, chloride and bicarbonate in which acetate is loaded with a ratio of $0.14 \cdot q_{max}$.

The additional required equations necessary to solve the system are the thermodynamic equilibrium that is used as calculated in Section 2.1 and 2.2. The simulation is done in COMSOL Multiphysics as explained in Section 3.7, in which the molalities are converted to mol/L to be solved in the software using the density of water (1 kg/L) and methanol (0.786 kg/L), respectively.

3. Materials and methods

3.1. Materials

Sodium bicarbonate was purchased from J.T. Baker. Anhydrous potassium acetate (99%), methanol (≥99.9%), dextran blue and anhydrous methanol (≥99.8%) were obtained from Sigma-Aldrich. Potassium chloride (> 99.5%) was purchased from Merck. Carbon dioxide (≥99.8%) was supplied by Linde as compressed gas. The strong anion exchange resin (Dowex Marathon MSA, macroporous) in the chloride form was purchased from Sigma Aldrich. The nominal total exchange capacity is at least 1.1 eq/L (wet basis). All aqueous solutions were prepared with deionized water from a Milli-Q water purification system (Millipore). Deionized water was used from a Milli-Q purification system.

3.2. Adsorption batch experiments

Adsorption experiments were performed in 50 mL flasks with 1 g of wet resin (chloride form) added to 10 mL aqueous solutions of a carboxylate salt/carboxylic acid at different concentrations. Sodium acetate solution concentrations were between 0.006 and 0.72 mol/kg (0.5–60 mg/$g_{solution}$), acetic acid between 0.012 and 3.66 mol/kg (0.7–180 mg/$g_{solution}$) and sodium bicarbonate between 0.006 and 0.34 mol/kg (0.5–28 mg/$g_{solution}$). The flasks were then shaken at 200 rpm and 25 °C for about 18 h in which equilibrium was reached (as checked with preliminary experiments). Each experiment was performed in duplicate. The pH of the samples before and after the reaction was measured. After the reaction each system was filtered using a Millex-GV Syringe Filter Unit and acetic acid, bicarbonate and chloride concentration in the liquid phase were quantified (Section 3.6).

3.3. Resin preparation for batch desorption

Column elution was used to convert the resin to the bicarbonate form. Fresh resin in the chloride form was hydrated in a beaker with deionized water for 30 min. The resin was then filtered under vacuum for 2 min in a glass filter. The hydrated resin was weighed and tightly packed in an Omnifit glass column (1 cm internal diameter, 15 cm height) and the column was placed in a Dionex Ultimate 3000 HPLC (Thermo Scientific). The resin was sequentially washed with 2 mL/min deionized water for 30 min, 4 mL/min sodium bicarbonate (20 g/L) for 240 min, then with 4 mL/min of deionized water for 240 min, and finally is converted to the acetate form with a solution of 0.10 mol/kg (10 g/L) potassium acetate at 2 mL/min. The absorbance of the outflow was continuously measured with the internal VWD-3400RS UV–Visible detector, and 2 mL samples were taken at 40 min intervals with the AFC-3000 automatic fraction collector. The last sample was analyzed for acetate concentration (Section 3.6). The breakthrough curve was constructed using the online measured absorbance and final sample acetate concentration, and the resin capacity for acetate was calculated by integration. The resin was removed from the column and washed 3 times with 50 mL deionized water and filtered at 20 mbar using Millipore Steriflip 60 µm nylon net filtration unit. The washing-filtering procedure was repeated two times with 30 mL of methanol and one time with 30 mL of anhydrous methanol. The resin was dried in an oven at 60 °C for 4 h to remove residual water and allow to cool in a desiccator.

3.4. Desorption batch experiments

Desorption experiments were performed at varying CO_2 pressures and methanol to resin ratios. CO_2 pressures of 2.1, 5, 10 and 20 bar and methanol to dry resin ratios of 5, 10, 15, 20, and 25 g/g were used. The desorption of acetate from the resin was performed by adding 0.5–2 g of resin (dry) and the required mass of anhydrous methanol in a 50 mL Büchi glass stirred autoclave. The (dry) resin has a water content of 8 w/w% as reported previously [3]. The vessel was equipped with a magnetically driven four blade impellers, an overhead motor, a pressure sensor, a pressure relief valve, a carbon dioxide inlet, and a sampling port. The reactor was flushed 4 times with CO_2. Agitation was set to 250 rpm and then CO_2 was added until the pressure stabilized at the desired value. The experiments were performed for 4 h in duplicate. Final pressure and temperatures (20–22 °C) were recorded. Liquid samples were obtained at the set pressure and analyzed for acetic acid concentration (Section 3.6).

3.5. Dynamic experiments

3.5.1. Dispersion and porosity determination

Hydrated resin was packed in an Omnifit glass column (15 cm height × 1 cm internal diameter). A 20 µL tracer pulse of aqueous potassium chloride (3 mol/L) was added at a constant flow (0.15–6 mL/min) to the system with (resin in chloride form) and without column at 20–22 °C. The mean time of passage (τ) and variance (σ^2) of the system with the column were calculated by numerical integration of the conductivity response, and used for the determination of total porosity as explained in Section 2.3. The particle porosity was measured in the system by repeating the experiment with 6.6 g/L of dextran blue as tracer.

3.5.2. Total resin capacity

The total anion exchange capacity of the resin was determined based on the ASTM D2187-94 Standard method-Test H. The method consists of the conversion of a sample to the chloride form using a concentrated solution of hydrochloric acid. The sample was washed with water and isopropanol. Elution of chloride from non-salt-splitting group was done using ammonium hydroxide. The sample was changed to the chloride form again washing it with sodium chloride (50 g/L) and the subsequent elution of chloride from salt splitting group was performed using sodium nitrate. Determination of chloride in the separate eluents was done by titration with silver nitrate (0.1 mol/L).

3.5.3. Adsorption dynamic experiments

An Omnifit glass column (1 cm internal diameter × 15 cm height) was used, with approximately 5 g of wet resin in the chloride form (~60 wt%/wt water). The dispersion of the column was measured as mentioned in Section 3.5.1. The column was converted to the bicarbonate form with a solution of 0.24 mol/kg (20 g/L) sodium bicarbonate (Section 3.3). Dynamic experiments were performed in a Thermo Scientific Dionex Ultimate 3000 system. Carboxylate solutions were pumped through the column at 0.3 and 2 mL/min and 25 °C. The carboxylate inlet solutions contained acetate 14.2 mmol/kg (0.84 g/L) and chloride 9 mmol/kg (0.32 g/L) at a pH of 5 or 7.6 Fractions of 2 mL were collected. Feed samples and collected fractions were analyzed for acetate and chloride, and pH, conductivity and absorbance (210 nm)

were measured online.

3.5.4. Desorption dynamic experiments

After an adsorption experiment, the column was washed with Milli-Q water (4 mL/min) until the conductivity was below 0.007 mS/cm. Then, the column was washed with methanol (2 mL/min) for 30 min. The desorption dynamic experiments were performed in a modified Thermo Scientific Dionex Ultimate 3000 system. The system was modified with a high-pressure pre-mixing vessel to equilibrate the methanol with 10 bar of carbon dioxide during ~30 min. A back-pressure was installed after all sensors to the modified system to assure that the pressure remained above the set-point of the pre-mixing vessel (10 bar). The methanol/carbon dioxide solution was pumped through the column at 1.5 mL/min at 20–22 °C. Fractions of 2 mL were collected. Collected fractions were analyzed for acetic acid as explained in Section 3.6, and absorbance (210 nm) was measured online.

3.6. Analytical methods

The concentration of total acetate in the systems was evaluated using a Waters HPLC system equipped with a UV/Visible Detector (Waters 2489) and a Refractive Index Detector (Waters 2414) for both water and methanol samples. The column used was the Bio-Rad Aminex HPX-87H column (7.8 × 300 mm). A mobile phase of phosphoric acid (1.5 mmol/L) was used in isocratic mode at 0.6 mL·min^{-1}. The injection volume was 10 µL and the duration of the run was 30 min, the column temperature was 60 °C and the detection was at 210 nm. The experimental aqueous acetate and acetic acid concentration were determined using the total acetate measurement, the experimental pH and Eq. (1). The methanol samples were diluted 10 times to avoid deterioration and interference with the column material. Chloride concentrations (Sigma-Aldrich MAK023) were determined spectrophotometrically using the Sigma Aldrich MAK023 test kit in 96 well plates. Total carbonate was measured as carbon dioxide with a Hach-Lange LCK388 kit, which includes all carbonate species (carbonate, bicarbonate and carbon dioxide).

3.7. Regression and model calculations

The determination of the parameters from each set of equations was done by minimizing the sum of mean squared error of the total acetate (chloride concentration for the bicarbonate experiment) with MATLAB® optimization algorithm *fminsearch*. The objective functions were the set of equilibrium equations that were solved in a separate MATLAB® function using the built-in nonlinear solver *fsolve*.

The dynamic model was implemented on the COMSOL Multiphysics platform (v5.2a, Comsol Inc., Burlington, MA). Equations for a one-dimensional dispersion and ion exchange were solved with a variable time step with a mesh size of $2 \cdot 10^{-4}$ m.

4. Results and discussion

4.1. Parameters for the ion exchange adsorption equilibrium model

Fig. 1 shows the isotherms for acetate, acetic acid and bicarbonate with the corresponding model. The maximum loading obtained was 169 mg/g (wet resin in chloride form) for acetate and 120 mg/$g_{wet\ resin}$ for acetic acid. Thus, the resin shows a lower capacity for acetic acid than for acetate. The bicarbonate isotherm does not reach a plateau because of low solubility of sodium bicarbonate (~1.3 mol/kg at 20 °C). The loading obtained for bicarbonate is 49 mg/$g_{wet\ resin}$. The total exchange capacity (q_{max}) was 1.9 mEq/$g_{wet\ resin}$, and measured as explained in Section 3.5.2. Some of the reported loadings for the adsorption of acid species with a quaternary group resin are: 24 mg/g $_{resin}$ for acetic acid with a Sepra SAX resin (silica matrix, quaternary amine group, 0% water), 66 mg/g $_{resin}$ for the Sepra ZT SAX resin (polymeric matrix with quaternary amine group, 0% water), and 41.2 mg/$g_{wet\ resin}$ on the A26OH resin (polystyrene matrix, quaternary ammonium group) [18–20]. In these reported values, the type of the functional group of the resin leads to different interactions of the functional group with the acid at the low pH experiments [21]. For the acetate recovery (pH above the pK_a), the obtained capacities are comparable with reported

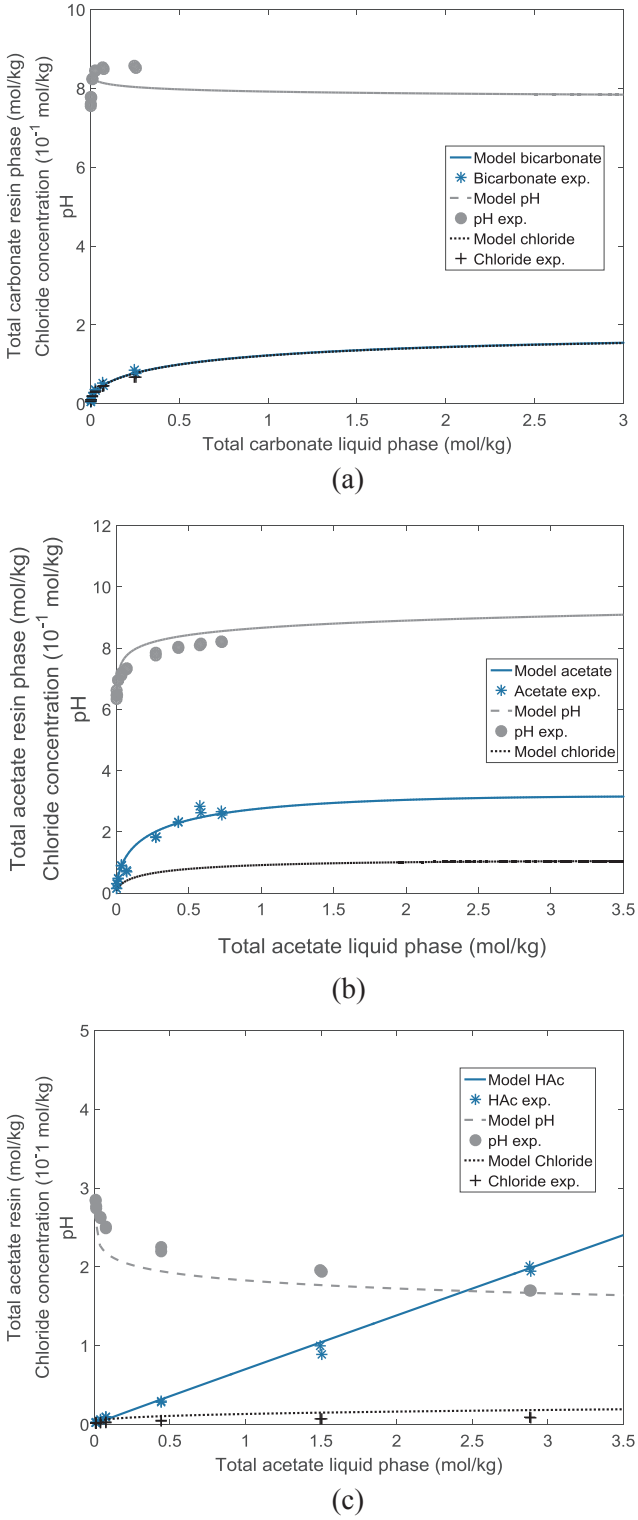

Fig. 1. Isotherms for (a) bicarbonate, (b) acetate and (c) acetic acid with Dowex MSA resin in the chloride form, experimental data (dots) and equilibrium model (lines). All experiments were performed with a ratio of 1 g of wet resin to 10 mL of solution.

values, 28 mg/$g_{wet\ resin}$ (IRA-910 chloride form) and 112 mg/$g_{wet\ resin}$ (IRA-910 hydroxide form) [22]. Experiments reported in dry resin basis were converted to wet basis assuming 60 wt.% water content.

Fig. 1 shows that the model follows the experimental values for chloride, bicarbonate, acetate and pH. The pH in all the experiments is lower than the pH of the feed solutions (data not shown), because chloride is a weaker base than bicarbonate and acetate. For acetic acid, which binds to the resin by hydrogen bonding [2], this was an indication that ion exchange also occurs, confirmed by the chloride release (Fig. 1c). The model could describe this behavior and the change of pH with an average error of 10.6% for total carbonate, 5.22% chloride and 4.92% for pH in the bicarbonate model (Fig. 1a); 5.6% acetate and 4.0% for the pH in the acetate model (Fig. 1b); 4.4% acetic acid, 9.6% for pH and a high error of 60% for the chloride in the acetic acid model (Fig. 1c). The high chloride error in the acetic acid model is assumed to be due to measurement error at these low concentrations (1–9 mmol/L). A reason for the discrepancy might be that the isotherms were not developed at isonormal conditions. Further studies should considered developing the isotherms at isonormal conditions to check if the correlation can be improved as reported by others [23].

The selectivity for acetate and bicarbonate over chloride and the overall distribution coefficient of acetic acid were estimated as: $K_{Cl^-}^{Ac^-} = 0.125$, $K_{Cl^-}^{HCO_3^-} = 0.206$ and $K_{OV,HAc} = 0.674\frac{\text{mol / kg}_{resin}}{\text{mol / kg}_{solution}}$. These parameters are comparable with reported values of 0.10 for the selectivity of acetate over chloride (calculated from their reported acetate/hydroxide and chloride/hydroxide selectivity) [24], 0.11–0.16 for propionate over chloride and 0.28 to 0.33 bicarbonate over chloride [25]. The selectivity of bicarbonate over chloride is lower than the one reported by others (0.21 compared to 0.23–0.33) [25]. The reason is that the equilibrium equation of carbon dioxide to carbonic acid (Eq. (3)) was added independently, and in other reported work [25] both equilibrium equations (Eqs. (3) and (4)) are included in one apparent equilibrium constant ($K_{app} = 6.3$). The resin supplier reports selectivity of 0.145 for acetate over chloride and 0.272 for bicarbonate over chloride [26]. Our distribution coefficient, of $K_{OV,HAc} = 0.674\frac{\text{mol / kg}_{resin}}{\text{mol / kg}_{solution}}$, for the acid species is higher than reported values with other strong anion exchange resins [24].

The obtained parameters values are used in Section 4.3 to build the dispersive-equilibrium model for the adsorption step.

4.2. Parameters for the desorption equilibrium model

In this section, the effect of excess methanol and CO_2 pressure in the desorption equilibrium of acetate from the strong anion exchange resin is studied. The aim is to estimate the parameter $K_{MeCO_3^-}^{Ac^-}$ required to describe the equilibrium reactions (as described in Section 2.2), and calculate the achievable dissolved acetic acid concentration after desorption. A series of batch desorption experiments at different pressures (2–20 bar) and methanol-to-resin ratios (5–25 g methanol/g resin (dry)) were performed with the resin in the acetate form. The equilibrium concentrations of acetic acid were determined for each experiment. The concentration values for the experiments at 2.1 bar CO_2 were used to determine the parameter for the model. The regressed parameter at 2.1 bar $pK_{MeCO_3^-}^{Ac^-}$, is 3.71 at 22 °C.

The error for the model at 2.1 bar ranges between 4.7% and 8.3%, with an average of 6.6%. The obtained $pK_{MeCO_3^-}^{Ac^-}$ value was used to predict the equilibrium desorption concentration at different pressures. The error of the predictions ranges from 0.9% to 10.8% with an average of 6.5% and 6.7% for 5 bar and 10 bar of CO_2, respectively. Additional experiments at 20 bar (5 and 30 g methanol per g of resin (dry)) were performed to check the validity of the model at higher pressures. The main deviations occur at high acetic acid concentration, and the reason may be that near-field binary and ternary interactions were not considered for the calculation of the activity coefficient (Section 2.2), which means that the model for activity coefficient calculations has the same accuracy as a Debye-Hückel model [15]. As well, high acetic acid concentrations imply high concentrations of dissolved CO_2 such that the activity coefficient might deviate and CO_2 might adsorb to the resin like acetic acid does.

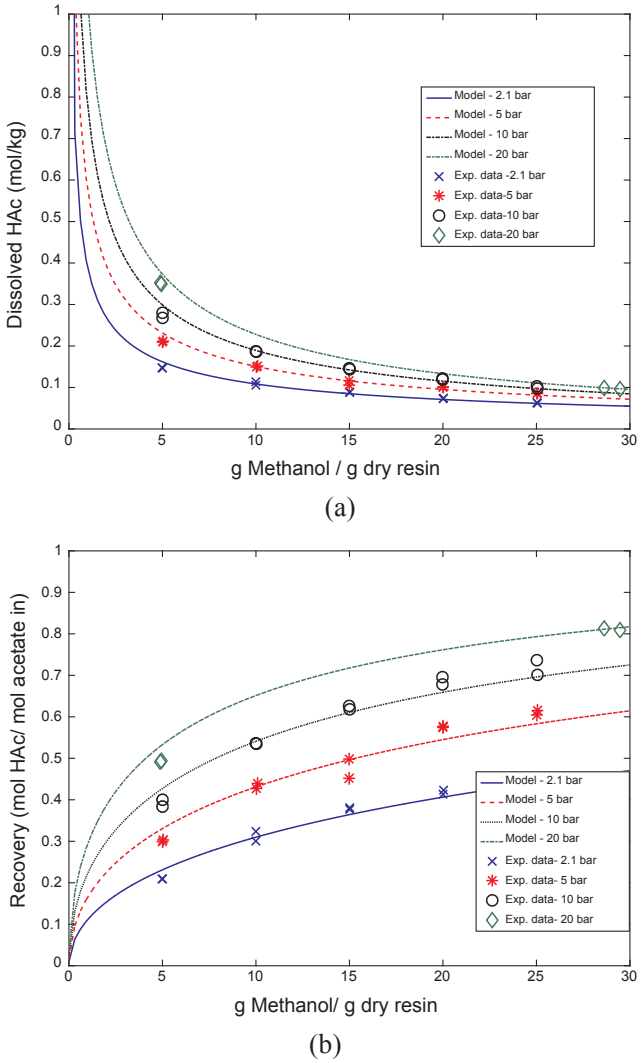

Fig. 2. Experiments results and model for the desorption equilibrium of acetate with CO_2-expanded methanol at 22 °C. (a) Acetic acid concentration as a function of the methanol/resin ratio, (b) acetate recovered from a fully loaded resin as a function of the methanol/resin ratio.

In Fig. 2, the experimental and predicted equilibrium concentrations and recoveries are presented. In Fig. 2a, the acetic acid equilibrium concentration is plotted as a function of the methanol/resin ratio for the four experimental CO_2 pressures. In Fig. 2b, the recovery (mol HAc in liquid/mol total acetate originally in resin) is presented as a function of the same variables. As expected, increasing the amount of methanol decreases the concentration of acetic acid but increases its recovery. As m_{MeOH} is constant, the concentration of methyl carbonate increases with CO_2 pressure. The ion exchange equilibrium is then displaced towards the acetate side, hence more acetic acid appears in solution. At 2.1 bar CO_2, reducing the methanol/resin ratio from 25 to 5 increases the dissolved HAc concentration from 0.063 to 0.147 mol/kg, but decreases the recovery (from 49.1 to 22.6%). That represents a 2.3-fold increase in concentration at the expense of a 2.2-fold decrease in recovery. At 5 bar CO_2, for the same decrease in the methanol/resin ratio, the concentration increases 2.47-fold at the expense of a 2.05 fold decrease in recovery. At 10 bar CO_2 the trade-off improves slightly; a 2.72-fold increase in concentration leads to a 2.02-fold decrease in recovery.

The effect of CO_2 pressure on concentration is more pronounced for lower methanol/resin ratios. However, it can be seen that as CO_2 pressure increases, its effect on both concentration and recovery levels off. Higher recoveries deplete the acetate bound to the resin, which in turn requires a larger concentration of methyl carbonate ions to achieve further desorption. The highest recovery achieved in this study is 81% when using 29 g_{MeOH}/g_{resin} and 20 bar CO_2. At these conditions, a concentration of acetic acid 0.098 mol/kg (4.6 g of acetic acid/L methanol) is obtained. This result is in line with Rebecchi et al., where 1 g of acid was desorbed with 0.2 L of basified ethanol (5 g of acid per L of ethanol) [18].

In Fig. 3, the model is used to extrapolate the results to 61 bar CO_2, where it becomes supercritical. The goal is to check the theoretical maximum concentration and recovery that can be achieved in one equilibrium stage. The recovery of acetate is plotted as a function of the equilibrium concentration for different methanol/resin ratios. Isobaric curves are also drawn to allow for a quick estimation of the recoveries and concentrations at different experimental conditions. The values are a useful approximation for design and operation of the column system.

The highest concentration is obtained at 61 bar, and it is about 0.48 mol/kg (22 g of acetic acid/L of methanol) with a recovery of about 70%. This indicates the possibility to increase the concentration in comparison with previous data [3,4]. However, lower pressures are desired for an industrial application. For this reason, a column operation (eventually a multicolumn system) is analyzed to improve the recovery further, which is studied in Section 4.3.

4.3. Equilibrium dispersive model for adsorption and desorption

Dynamic adsorption experiments were performed at different flows (0.3 and 2 mL/min) and different feed pH (5 and 7.6) with the resin initially in the bicarbonate form. The results are shown in Fig. 4.

Fig. 4 confirms that chloride is more selective to the ion exchange resin than acetate. This causes an overshooting of acetate after the breakthrough of chloride (Fig. 4a), in line with data for recovery of carboxylates from paper mill wastewater [4]. In general, overshooting of an ion occurs when the feed solution contains ions with higher selectivity for the resin group than the overshot ion, resulting in a portion of eluted solution with a concentration of the latter above its feed concentration [27].

At pH 5, the loading of total acetate to the resin is higher, caused by the additional adsorption of acetic acid to the backbone of the resin. Additionally, a lower elution of bicarbonate at pH 5 than at pH 7 supports the hypothesis that part of the total acetate is removed by hydrophobic adsorption and not by ion exchange.

An equilibrium dispersive model was used to study the behavior of the adsorption to the column in the bicarbonate form. Fig. 4 shows that the model represents the expected trends for all species. The equilibrium constant (selectivity) of acetate over bicarbonate was calculated from the values obtained of acetate over chloride and bicarbonate over chloride (Section 4.1). The model presents deviations caused by the assumptions used to simplify the system, namely: equal dispersion coefficient for all compounds, all mass transfer effects lumped into the dispersion coefficient, the bed void fraction calculated using dextran blue, and negligible concentrations of carbonate and carbonic acid. The apparent dispersion coefficient was calculated, as mentioned in Section 2.3, using Eq. (29). To improve the model, one might use correlations for the lumped dispersion coefficient that take into account diffusion rates into the particles. Bicarbonate was the species that has the highest deviation from the model. Main reasons can be experimental variations caused by measurement errors (inaccuracy of the carbonate measurement method), and the fact that divalent carbonate was not considered in the model.

The dynamic desorption experiments are shown in Fig. 5. For these experiments, the resin is pre-loaded with an acetate and chloride solution (as in the dynamic adsorption experiments), or fully pre-loaded with acetate. For the resin pre-loaded with acetate and chloride, the resin had all three anions (acetate, chloride and bicarbonate) prior to desorption. The ratio of acetate on the resin compared with the total resin capacity was 0.14. The desorption was performed using CO_2-expanded methanol pre-equilibrated at 10 bar at an operational pressure of 31 bar in the column controlled by the back-pressure. The maximum experimental concentration of acetic acid achieved was 0.427 mol/kg (20 g/L_{MeOH}), which indicates that the CO_2 concentration is dictated by the operation pressure (31 bar), since the maximum expected methyl carbonic acid concentrations are 0.183 mol/kg (at 10 bar of CO_2) and 0.515 mol/kg (at 31 bar of CO_2), calculated from the methyl carbonic acid concentration of the equilibrium reactions (Section 4.2). All the equilibrium constants (K_{ACA}, $K^{Ac^-}_{MeCO_3^-}$, K_m) were combined to represent the equilibrium as one reaction with a constant of 1.97 (Appendix A.5). In this way, dissolved ions were not taken into account, which can be justified because their proportion was relatively low.

The CO_2-expanded methanol cannot desorb bound chloride. This is confirmed by the loss of acetate capacity after several adsorption and desorption cycles (Appendix A.6). The reason that chloride cannot be desorbed is because of its low pK_m (pK_a of HCl in water is −5.9) [28].

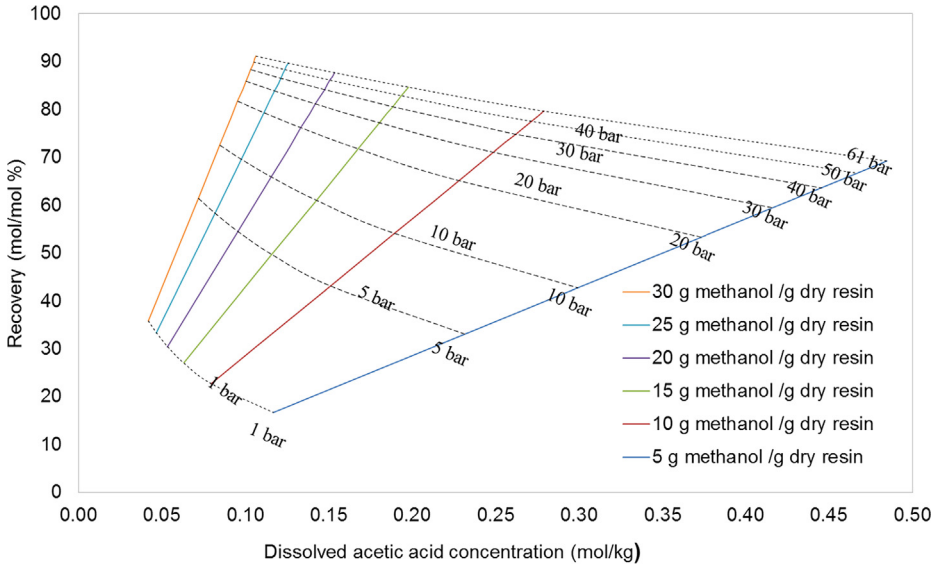

Fig. 3. Recovery of acetic acid as a function of the equilibrium acetic acid concentration for different methanol/resin ratio. The dotted lines represent isobaric curves.

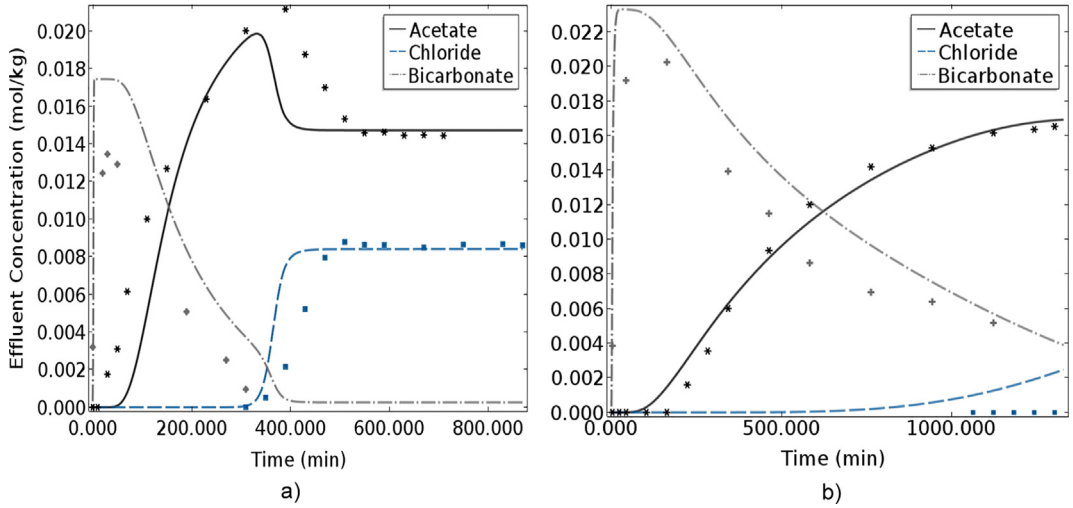

Fig. 4. Dynamic ion exchange adsorption of acetate and chloride at a flow rate of 2 mL/min and a pH of 5 (a), and a flow rate of 0.3 mL/min and a pH of 7 (b). The feed solution has a concentration of 14.4 mmol/kg of acetate and 8.91 mmol/kg of chloride, the resin was preloaded with bicarbonate. Markers are experimental data, the model is represented by lines.

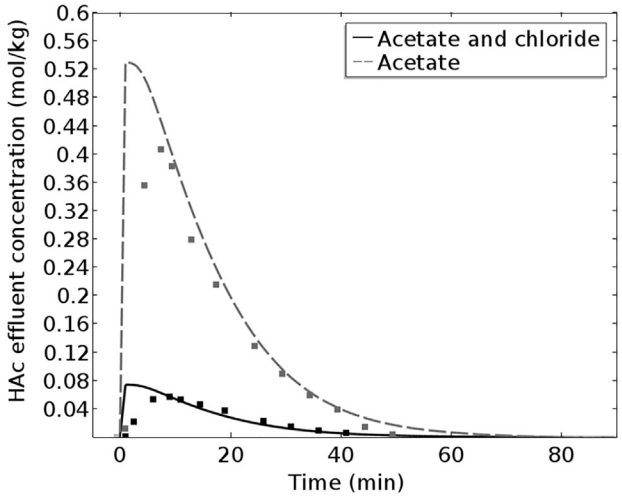

Fig. 5. Dynamic CO_2-expanded methanol desorption of acetate at 31 bar operation pressure for resin pre-loaded with acetate or with a mixture of acetate and chloride. Markers are experimental data, the model is represented by lines.

To remove the chloride, the resin was additionally regenerated using an aqueous bicarbonate solution.

For the resin loaded with acetate and chloride, the inlet concentration of methyl carbonic acid was assumed to be the ratio of acetate bound to the resin and the concentration of methyl carbonic acid ($0.14 * m_{HMeCO_3}$) at the operating pressure of 31 bar. The reason was that methyl carbonate seemed to exchange not only with acetate, but also with the bicarbonate bound to the resin. This caused a higher consumption of methyl carbonic acid than the expected if only acetate was on the resin. To prove this, the resin was fully pre-loaded with acetate instead of an acetate-chloride solution. Fig. 5 shows that the model presents a trend closer to these experimental data. This states the importance of having a fully pre-loaded resin during desorption, which is comparable to other desorption-reaction techniques [29].

The dispersion coefficient of the desorption step was fitted to the fully loaded acetate experiment and was not calculated using empirical correlations. A more detailed study of the dispersion coefficient of desorption with CO_2-expanded methanol is needed.

The equilibrium and the dynamic experiments show that the resulting concentration of acetic acid in CO_2-expanded methanol is limited by the methyl carbonic acid concentration. The actual column system presents an improvement from our previous reported data, from 0.8 to 2.4 g/L to 20 g/L HAc, and the model can be used to design a simulated moving bed multicolumn system. A multicolumn system can improve the total resin usage and the breakthrough capacity can be increased [30], but the concentration of HAc remains limited by the methyl carbonic acid concentration (pressure of CO_2) and ratio between acetate and other anions in the resin. It would be useful to extend the proposed model to the desorption of mixtures of organic acids, as they are commonly encountered in fermentation and acidogenic anaerobic digestion.[18]

5. Conclusions

This chapter presented an equilibrium-dispersive model to describe and validate the recovery of acetate by anion exchange with a consecutive desorption with CO_2-expanded methanol. The equilibrium parameters were estimated as: $K_{Cl^-}^{Ac^-} = 0.125$, $K_{Cl^-}^{HCO_3^-} = 0.206$ and $K_{OV,HAc} = 0.674 \frac{\text{mol / kg}_{\text{resin}}}{\text{mol / kg}_{\text{solution}}}$ for batch adsorption, and $\text{p}K_{MeCO_3^-}^{Ac^-} = 3.71$ for batch desorption. Using these parameters, the maximum equilibrium concentration of acetic acid (after batch desorption) was predicted to be 0.48 mol/kg at 61 bar. The dynamic behavior for all species were described using the equilibrium-dispersive model. For column adsorption, it was concluded that acetic acid also binds to the resin, since there was a higher loading of total acetate at pH 5 in comparison with pH 7, complemented with a lower elution of bicarbonate. Additionally, the higher selectivity of chloride in comparison to acetate caused an overshooting of acetate. For column desorption, it was concluded that the acetic acid concentration in the CO_2-expanded methanol was limited by the methyl carbonic acid concentration and the ratio of acetate to chloride loaded to the resin. The maximum achieved acetic acid concentration was 0.427 mol/kg (20 g/L_{MeOH}) at an operating pressure of 31 bar. The concentrations reported in this chapter are an improvement from previous reported data. The model presented the equilibrium and dispersive parameters required to design the specific columns within a multicolumn operation scheme.

Acknowledgements

This research was financed by the Netherlands Organisation for Scientific Research (NWO) domain Applied and Engineering Sciences (TTW) and Paques B.V. partnership: The Volatile Fatty Acid Platform.

Appendix A. Supplementary material

Supplementary data associated with this article can be found, in the online version, at https://doi.org/10.1016/j.seppur.2018.03.068.

References

[1] Y. Chen, J. Nielsen, Biobased organic acids production by metabolically engineered microorganisms, Curr. Opin. Biotechnol. 37 (2016) 165.
[2] C.S. López-Garzón, A.J.J. Straathof, Recovery of carboxylic acids produced by fermentation, Biotechnol. Adv. 32 (2014) 873.
[3] C.I. Cabrera-Rodriguez, L. Paltrinieri, L.C.P.M. de Smet, L.A.M. van der Wielen, A.J.J. Straathof, Recovery and esterification of aqueous carboxylates by using CO_2-expanded alcohols with anion exchange, Green Chem. 19 (2017) 729.
[4] C.I. Cabrera-Rodríguez, M. Moreno-González, F.A. de Weerd, V. Viswanathan, L.A.M. van der Wielen, A.J.J. Straathof, Esters production via carboxylates from anaerobic paper mill wastewater treatment, Bioresource Technol. 237 (2017) 186.
[5] J.-R. Bastidas-Oyanedel, F. Bonk, M.H. Thomsen, J.E. Schmidt, Dark fermentation biorefinery in the present and future (bio)chemical industry, Rev. Environ. Sci. Bio/Technol. 14 (2015) 473.
[6] C.N. Fredd, H. Scott Fogler, The kinetics of calcite dissolution in acetic acid solutions, Chem. Eng. Sci. 53 (1998) 3863.
[7] L.N. Plummer, E. Busenberg, The solubilities of calcite, aragonite and vaterite in CO_2-H_2O solutions between 0 and 90 °C, and an evaluation of the aqueous model for the system $CaCO_3$-CO_2-H_2O, Geochim. Cosmochim. Acta 1011 (1982) 46.
[8] P.F. Lito, S.P. Cardoso, J.M. Loureiro, C.M. Silva, Ion exchange equilibria and kinetics, in: I. Dr, M. Luqman (Eds.), Ion Exchange Technology I: Theory and Materials, Springer, Netherlands, Dordrecht, 2012, p. 51.
[9] J.P.S.C. Aniceto, P. Simão, Tiago L. Faria, Patrícia F. Lito, Carlos M. Silva, Modeling ion exchange equilibrium: analysis of exchanger phase non-ideality, Desalination 290 (2012) 43.
[10] J.F. Pankow, Aquatic Chemistry Concepts, Lewis Publishers, Chelsea, Michigan, 1991.
[11] B.S. Vo, D.C. Shallcross, Modeling solution phase behavior in multicomponent ion exchange equilibria involving H^+, Na^+, K^+, Mg^{2+}, and Ca^{2+} ions, J. Chem. Eng. Data 2005 (1995) 50.
[12] A.H. Truesdell, B.F. Jones, WATEQ, a computer program for calculating chemical equilibria of natural waters, J. Res. US Geol. Surv. 2 (1974) 233.
[13] J.L. Gohres, A.T. Marin, J. Lu, C.L. Liotta, C.A. Eckert, Spectroscopic investigation of alkylcarbonic acid formation and dissociation in CO_2-expanded alcohols, Ind. Eng. Chem. Res. 48 (2009) 1302.
[14] E.L.M. Miguel, P.L. Silva, J.R. Pliego, Theoretical prediction of pKa in methanol: testing SM8 and SMD models for carboxylic acids, phenols, and amines, J. Phys. Chem. B 118 (2014) 5730.
[15] J. Gmehling, B. Kolbe, M. Kleiber, J. Rarey, Chemical Thermodynamics for Process Simulation, Wiley-VCH, Weinheim, Germany, 2012.
[16] G. Carta, A. Jungbauer, Protein Chromatography: Process Development and Scale-up, Wiley-VCH, Weinheim, 2010.
[17] H. Schmidt-Traub, M. Schulte, A. Seidel-Morgenstern, Preparative Chromatography, second ed., Wiley, Weinheim, 2012.
[18] S. Rebecchi, D. Pinelli, L. Bertin, F. Zama, F. Fava, D. Frascari, Volatile fatty acids recovery from the effluent of an acidogenic digestion process fed with grape pomace by adsorption on ion exchange resins, Chem. Eng. J. 306 (2016) 629.
[19] C. Fargues, R. Lewandowski, M.-L. Lameloise, Evaluation of Ion-exchange and adsorbent resins for the detoxification of beet distillery effluents, Ind. Eng. Chem. Res. 49 (2010) 9248.
[20] A.H. da Silva, E.A. Miranda, Adsorption/desorption of organic acids onto different adsorbents for their recovery from fermentation broths, J. Chem. Eng. Data 58 (2013) 1454.
[21] P. Gluszcz, T. Jamroz, B. Sencio, S. Ledakowicz, Equilibrium and dynamic investigations of organic acids adsorption onto ion-exchange resins, Bioprocess Biosyst. Eng. 26 (2004) 185.
[22] H. Reisinger, C.J. King, Extraction and sorption of acetic acid at pH above pKa to form calcium magnesium acetate, Ind. Eng. Chem. Res. 34 (1995) 845.
[23] G.J. Millar, S.J. Couperthwaite, C.W. Leung, An examination of isotherm generation: impact of bottle-point method upon potassium ion exchange with strong acid cation resin, Sep. Purif. Technol. 141 (2015) 366.
[24] M.L. Jansen, J. Houwers, A.J.J. Straathof, L.A.M. van der Wielen, K.C.A.M. Luyben, W.J.J. van den Tweel, Effect of dissociation equilibria on ion-exchange processes of weak electrolytes, AIChE J. 43 (1997) 73.
[25] N. Kanazawa, K. Urano, N. Kokado, Y. Urushigawa, Adsorption equilibrium equation of carboxylic acids on anion-exchange resins in water, J. Colloid Interface Sci. 238 (2001) 196.
[26] Dow Using Ion Exchange Resin Selectivity Coefficients. 30/06/2017. < http://msdssearch.dow.com/PublishedLiteratureDOWCOM/dh_0988/0901b803809885be.pdf?filepath=liquidseps/pdfs/noreg/177-01755.pdf&fromPage=GetDoc > .
[27] G. Crini, P.M. Badot, Sorption Processes and Pollution: Conventional and Non-conventional Sorbents for Pollutant Removal from Wastewaters. Presses universitaires de Franche-Comté, 2010.
[28] A. Trummal, L. Lipping, I. Kaljurand, I.A. Koppel, I. Leito, Acidity of strong acids in water and dimethyl sulfoxide, J. Phys. Chem. A 120 (2016) 3663.
[29] C.I. Cabrera-Rodríguez, L.A.M. van der Wielen, A.J.J. Straathof, Separation and catalysis of carboxylates: byproduct reduction during the alkylation with dimethyl carbonate, Ind. Eng. Chem. Res. 54 (2015) 10964.
[30] H. Nagai, G. Carta, Lysine adsorption on cation exchange resin. iii. multicolumn adsorption/desorption operation, Sep. Sci. Technol. 40 (2005) 791.